Performance and adaptive value of tarsal morphology in rove beetles of the genus *Stenus* (Coleoptera, Staphylinidae)

Oliver Betz*

Zoologisches Institut der Universität, Ökologie, Olshausenstraße 40, D-24098 Kiel, Germany

*e-mail: obetz@zoologie.uni-kiel.de

Summary

To evaluate the adaptive value of the widening of the bilobed tarsi that has paralleled the tremendous radiation of the staphylinid genus *Stenus*, the performance of slender *versus* wide tarsi has been evaluated in two different contexts: (i) locomotion on the surface of water, and (ii) climbing on vertical (plant) surfaces. Contact angle measurements at the underside of the tarsi have revealed that, irrespective of tarsus width, all the investigated species are well supported by the surface of water while walking on it. The main selective demands driving the widening of the tarsi in several lineages have instead come from their firm attachment to smooth plant surfaces. This is suggested by measurements of the maximum vertical pulling forces exerted by intact and manipulated individuals on various rough and smooth surfaces. Species with widened tarsi associated with considerably more tenet setae attain significantly higher pulling forces, particularly on smooth surfaces. The tarsal setae are of greater importance on smooth surfaces, but the claws seem to be more important on rough substrata. On substrata that combine the attributes of rough and smooth surfaces, both claws and tenent setae add significantly to the pulling forces exerted, suggesting a functional synergism. The contribution of the present study to our understanding of insect tarsal attachment to surfaces with a variety of textures is discussed.

Key words: adhesion, climbing, ecomorphology, locomotion, tarsus, tenent seta, water surface, rove beetle, staphylinid, *Stenus*.

Introduction

The demands on insect tarsi to meet adhesive requirements while walking on smooth (plant) surfaces have been realized *via* two different evolutionary pathways (Hasenfuss, 1999), which can be designated as 'hairy' *versus* 'smooth' systems (Jiao et al., 2000): (i) arrays of ventral tarsal tenent setae, and (ii) large areas of smooth flexible cuticle as manifest in the euplantulae or arolia. In the vast majority of lineages in the Coleoptera, only the first, 'hairy', system has evolved, giving rise to a large diversity of setal structure (Stork, 1980b). Most studies on the mechanism of insect tarsal attachment to the substratum have focused on single species (e.g. Dixon et al., 1990; Lees and Hardie, 1988; Stork, 1980a); only a few studies have approached this subject in a comparative way to evaluate the biological roles of specific tarsal morphologies (e.g. Federle et al., 2000; Gorb et al., 2001). However, from an ecomorphological point of view (e.g. Bock, 1988, 1990), such investigations should contribute to our understanding of the adaptive values of specific tarsal designs and their underlying selective pressures. The present analysis compares tarsal performance in representatives of various rove beetle species of the genus *Stenus*. This analysis is based on a previous study describing the main functional elements of the tarsi in this group of beetles, i.e. pretarsus including claws, tenent setae and tarsal secretion (Betz, 2002).

Rove beetles of the genus *Stenus* Latreille are well known because of their protrusible prey-capture apparatus (e.g. Betz, 1996; Weinreich, 1968), which must be considered a key innovation responsible for the tremendous radiation of this genus (more than 2100 species worldwide) (see Herman, 2001). This radiation has taken place with significant variation in the structure of the tarsi, which may be (i) slender with weakly or non-bilobed tarsomeres (subgenera *Stenus* s. str., *Nestus* and *Tesnus*) or (ii) widened with distinctly bilobed tarsomeres (subgenera *Hypostenus*, *Metastenus* and *Hemistenus*) (see fig. 1 in Betz, 2002) (Freude et al., 1964; Puthz, 1971). Morphometric analyses have shown that these two groups are clearly distinct in that wide bilobed tarsi can accommodate significantly more ventral tarsal setae than can slender tarsi (Betz, 2002). On the basis of outgroup comparisons, slender tarsi in the listed subgenera very probably represent the ancestral state of these beetles (V. Puthz, personal communication), whereas wide bilobed tarsi may have evolved as a derived state in the context of plant climbing, opening a novel adaptive zone for this group of organisms. This hypothesis is supported by the observation that, at least in central Europe, *Stenus* species with slender tarsi are soil dwellers, whereas species with wide tarsi are predominantly plant-climbers (Betz, 1998a,b).

However, behavioural observations have revealed that representatives of ground-dwelling species with slender tarsi are also capable of climbing up the lower parts of vegetation, e.g. for foraging or finding shelter at night (Betz, 1994). Moreover, at least in the temperate zones, most of the species appear to be associated with wetlands (e.g. Anderson, 1984; Horion, 1963; Koch, 1989; Puthz, 1971; Renkonen, 1934), where they inhabit waterside environments such as reeds or sparsely vegetated sites on river or lake margins. In these habitats, the representatives of many species can regularly be observed voluntarily walking across the surface of water supported only by their tarsi (Betz, 1999). Since this support depends on the contact between the entire tarsus and the water surface (e.g. Denny, 1993; Guthrie, 1989), it can be hypothesized that species with wide bilobed tarsi are better adapted to this mode of locomotion than species with slender tarsi (see Renkonen, 1934).

I have therefore tested two alternative hypotheses to explain the primary biological role of widened bilobed tarsi in this group of organisms: (i) that widened tarsi allow better adhesion to smooth (plant) surfaces and thus more effective climbing in the (reed) vegetation and (ii) that widened tarsi provide better support on the water surface as a precondition for successful colonization of waterside wetland habitats. I have tested these hypotheses experimentally (i) by analyzing the vertical climbing performance of 18 *Stenus* and one species of the sister genus *Dianous* on differently textured surfaces using a microbalance (similar to the experimental design used previously) (see Stork, 1980a), and (ii) by measuring the contact angles at the interface between the water and the ventral tarsus surface to calculate the vertical upward component of the surface tension supporting the body weight of the beetle. Experiments eliminating either the tarsal claws or the tenent setae have provided additional insights into the underlying mechanisms of tarsal attachment and the functional roles played by both these elements on various surface structures.

Materials and methods

Experiment 1: interspecific comparison of vertical climbing performance on a variety of surfaces

These experiments were conducted with 10 individuals (five males, five females) of each of the 18 *Stenus* species and one *Dianous* species (listed in Table 2). The beetles were anaesthetized with CO_2, and a stiff hair (twice as long as the beetle) was glued longitudinally to the surface of the pronotum. During 1 day of recovery, the beetles were kept on clean moist filter paper. Immediately prior to the experiments, each beetle was weighed, and the free end of the hair was fixed to a small mount. The mount and beetle were placed on the scale of a microbalance (Research R 160 P, Sartorius, Göttingen, Germany) so that the beetle was oriented upright (perpendicular to the ground) without tarsal contact with a solid surface. After zeroing the balance, a microscope slide, on which the surface to be tested had been fixed, was smoothly brought close to the ventral side of the beetle. As soon as the beetle had contacted the surface, it tried to climb upwards but

was held back by the weight of the mount. The corresponding negative mass readings of the microbalance (i.e. the mass pulled by the beetle) were continuously and automatically recorded ($20\,s^{-1}$) for 405 s and transferred to a computer system (Balread, Sartorius, Göttingen, Germany).

The pulling forces produced by the beetles were calculated by multiplying these masses by gravitational acceleration. As a result, characteristic traces were obtained showing the pulling forces continuously exerted by the individual beetles throughout the experiment (Fig. 1). For further comparative analyses, only the maximal force was selected in each case. Since the microbalance was set to its lowest sensitivity to external vibrations, the recorded maxima accurately reflect the actual maximum pulling performance of the beetles. By direct observation of the beetles during the experiments, it could be confirmed that they actually exhibited their maximum pulling performance, i.e. they attempted to escape from the fixed mount by pulling vertically in the direction of maximum sensitivity of the balance. This could be further ensured by occasionally stroking the beetle with a fine hairbrush to stimulate escape behaviour.

The vertical climbing performance of each beetle was tested on four different surfaces, with approximately 3 h of recovery between tests (Fig. 2): (i) factory-cleaned microscope glass slides (Wetzel, Braunschweig, Germany) (Fig. 2A); (ii) undeveloped fibre-based non-glossy photographic paper (RC DeLuxe Multigrade III, Ilford, UK) (Fig. 2B); (iii) the adaxial surface of young air-dried reed leaves (*Phragmites communis* Trin.) (Fig. 2E); (iv) thin filter paper (Fig. 2F).

Experiment 2: measurement of the relative significance of tarsal claws versus *tenent setae for vertical climbing on a variety of surfaces*

For these experiments, I compared *S. comma* (slender tarsi) with *S. pubescens* and *S. cicindeloides* (both with wide bilobed tarsi). Apart from the above-mentioned surface types i, iii and
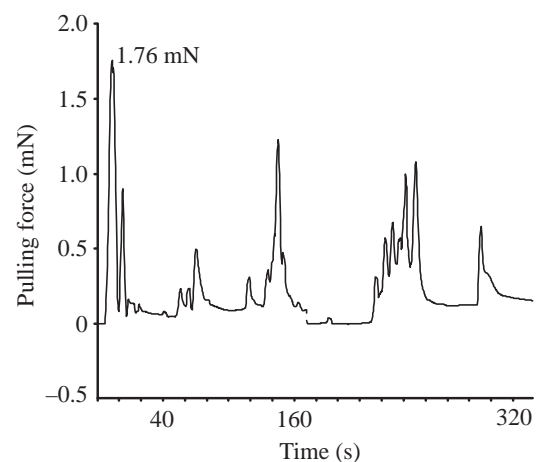
Fig. 1. Representative example of the continuously recorded pulling force exerted by an individual beetle (*Stenus pubescens*) on a dry reed (*Phragmites*) surface. The maximal attained pulling force is indicated.

iv, additional tests were performed with *S. comma* and *S. pubescens* but only on the adaxial surfaces of young fresh leaves of (v) *Glyceria maxima* (C. Hartm.) Holmb. (Fig. 2C) and (vi) *Phragmites communis* (Fig. 2D). The surface of *Phragmites* leaves undulates on account of the protruding parallel veins, but *Glyceria* leaves have much smoother surfaces.

For each species, two groups of 10 beetles (each consisting of five males and five females) were tested. After the pulling forces of all 20 intact beetles had been measured as described above, the beetles were anaesthetized and, in the first group of 10 individuals, the claws of the forelegs were cut at the base, and in the second group, the tarsal tenent setae were 'neutralized' by covering them with a thin layer of fast-drying superglue. The latter formed a smooth hard layer covering tarsomeres I–IV; tarsomere V with the claws remained intact.
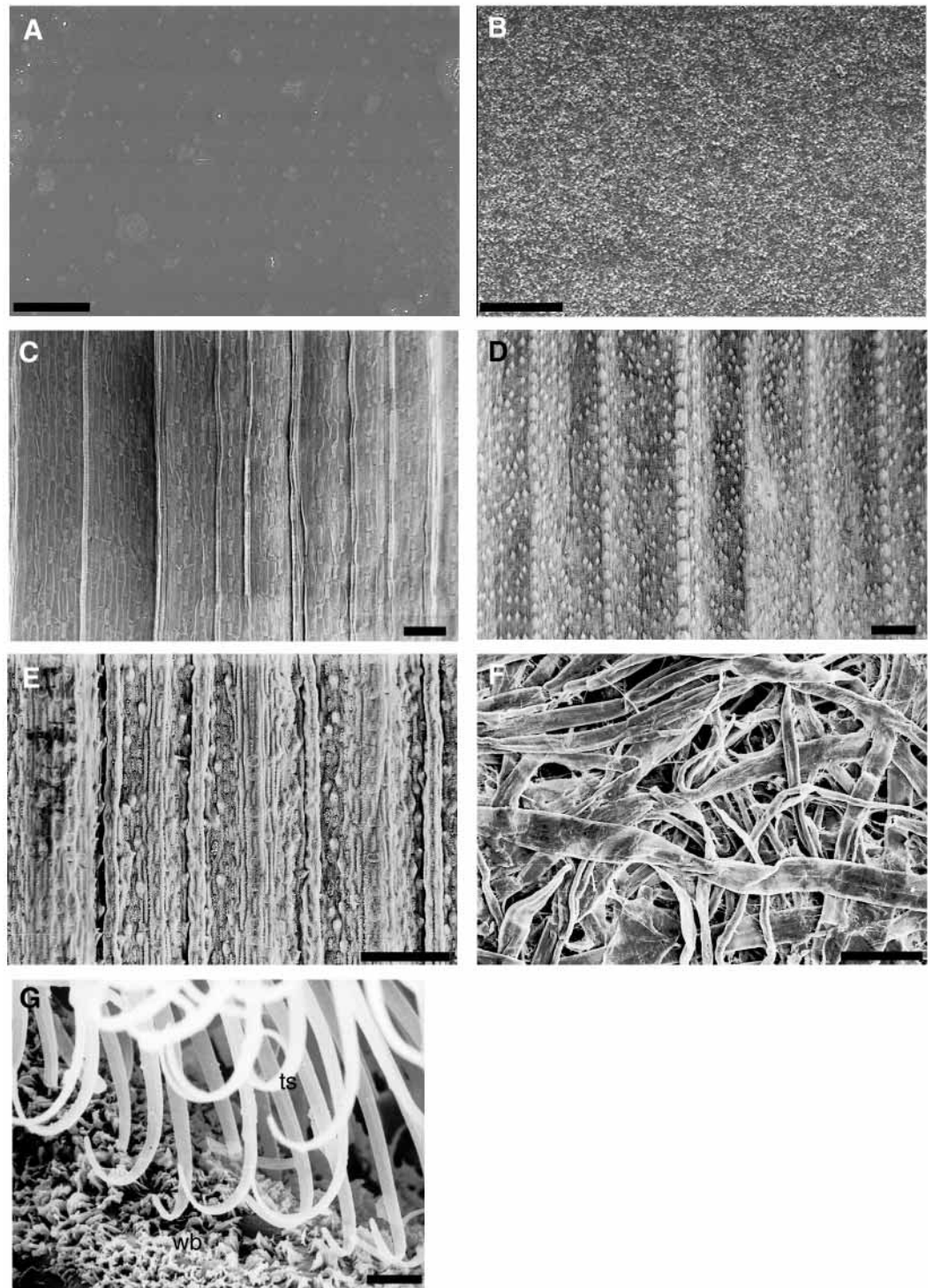

Fig. 2. Scanning electron micrographs of the surfaces used for the measurements of the pulling forces of the beetles: (A) a glass microscope slide, (B) photographic paper, (C) a fresh leaf of *Glyceria maxima*, (D) a fresh and (E) a dry leaf of *Phragmites communis* and (F) filter paper. (G) Lateral view of the contact zone between the tarsal tenent setae (ts) of tarsomere IV of *Stenus pubescens* and a dry *Phragmites* leaf. Scale bars: A–F, 100 µm; G, 3 µm. The plant surfaces represent the adaxial surfaces of young (uppermost) leaves of plants collected in the field. Fresh leaves of *Glyceria maxima* and *Phragmites communis* were observed directly using low-voltage scanning electron microscopy, whereas all the other surfaces were air-dried and gold-coated before examination at high voltage. wb, wax blooms.

The superglue treatment was not applied to the articulation zones between the single tarsomeres so it did not reduce the mobility of the tarsomeres relative to each other. After 1 day of recovery with food *ad libitum*, the pulling forces on the various surfaces were measured again in both groups under otherwise identical conditions.

Measurement of the surface roughness of a variety of surfaces

The four test surfaces used in experiment 1 were sputter-coated with gold to increase their reflection during the following measurements. The surface roughness (*Ra* values) was determined with an optical profiler (Veeco Instruments Inc., type NT3300), which was run in the VSI mode and calibrated according to an NIST-certified step height standard (10.10 μm step height). To equalize possible tilts of the test surfaces, one layer was subtracted from the measured surface images prior to the determination of their roughness.

Measurement of the apparent surface energies of a variety of surfaces

The apparent surface energies of the majority of test surfaces were determined by measuring the advancing contact angle with a drop shape analysis system (DSA 10-G140, Krüss GmbH, Hamburg, Germany) using water and di-iodomethane as test liquids (volume flux $10\,\mu\mathrm{l\,min^{-1}}$, conic calculation method). On account of the considerable undulation of the dry surface of *Phragmites*, the contact angle on this surface was measured statically, whereas it was measured dynamically (sessile drop method) on all the other surfaces. The apparent surface energies (made up of their polar and dispersive components) were automatically calculated by the system according to Owens and Wendt (1969) and Rabel (1971) from the drop shape data.

Measurement of the surface tension of pond water

Samples of pond water from two different locations near Kiel (Northern Germany), where *Stenus* beetles were observed to be active on the surface of the water, were taken in August. The surface tension was measured in the laboratory with a processor tensiometer (K12, Krüss, Hamburg, Germany) as $70.5\,\mathrm{mN\,m^{-1}}$ at 27.4 °C and $66.4\,\mathrm{mN\,m^{-1}}$ at 26.6 °C.

Qualitative demonstration of non-wettable and wettable parts of the body during locomotion on the surface of water

A test chamber ($3\,\mathrm{cm}\times2\,\mathrm{cm}\times1.5\,\mathrm{cm}$) with white-coloured inner sides was filled with tap water (surface tension $72.0\,\mathrm{mN\,m^{-1}}$) according to Baudoin (1976). The surface of the water was illuminated by fibre optics from an angle of approximately 70°. Beetles from various subgenera with slender tarsi (*S. comma*, *S. juno*, *S. boops*) and wide tarsi (*S. cincindeloides*, *S. solutus*, *S. pubescens*) were observed while walking on the surface of the water in this container. The shadows on the bottom of the container produced by those parts of the body that contacted the surface of the water were recorded by a video system. Depressions caused by the weight of the beetle pressing down the water surface *via* hydrophobic body surfaces gave large roundish shadows at the bottom of the test chamber, whereas upward-curving menisci caused by hydrophilic surfaces produced luminous points (Baudoin, 1976).

Quantification of the wettability of the ventral side of the tarsi

The wettability of the ventral side of the tarsi by water was determined in 4–5 specimens of each of six equally sized *Stenus* of various subgenera with slender or wide tarsi and in one *Dianous* species with slender tarsi. The animals were anaesthetized with CO_2, decapitated and fixed on their back on a mechanical stage. The advancing apparent contact angles between the ventral sides of the middle tarsi and distilled water were measured dynamically using the drop shape analysis system described above. The vertical component of the surface tension F_S acting on the ventral tarsal surface and supporting the insect on the surface of water was calculated according to Baudoin (1976) and Guthrie (1989) as:

$$F_S = c\gamma\cos\psi, \qquad (1)$$

where c is the line of contact of the ventral tarsal surface (the perimeter of the leg–water interface), γ is the surface tension of the water and ψ is the angle at which the vertical component of the surface tension acts. Since the tarsi rest flat upon the surface of water, their line of contact c was treated as being rectangular (see Suter and Wildman, 1999) and approximated as:

$$c = 2(T_1 + T_w), \qquad (2)$$

where T_1 and T_w are the mean tarsal length and width, respectively. The angle θ was calculated as:

$$\psi = 180 - \theta, \qquad (3)$$

where θ is the measured apparent contact angle between the ventral side of the tarsi and the water.

A safety coefficient C, estimating the capacity of the buoyancy plus surface tension to support the beetle on the surface of the water, was calculated according to Baudoin (1976):

$$C = 3(F_S + F_B)/w, \qquad (4)$$

where F_B is the buoyancy and w is the body weight of the beetles. The factor 3 was used to meet the condition that, during normal locomotion on the water surface, only three tarsi might be in contact with the water at any time (Betz, 1999). The buoyancy was approximated as:

$$F_B = \pi r^2 l\rho g, \qquad (5)$$

assuming that the tarsi, while resting flat upon the surface of the water, form a cylinder with a radius r and length l (both species-specific), which displaces an equal amount of water with a density ρ of $1\,\mathrm{kg\,m^{-3}}$; g is gravitational acceleration, i.e. $9.81\,\mathrm{m\,s^{-2}}$.

Scanning electron microscopy

To measure the morphometric parameters of the tarsi of the various species as required for the above calculations, whole

legs were stepwise dehydrated in ethanol/acetone, critical-point-dried (CPD 020, Balzers, Germany), fixed to stubs with silver paint, coated with gold (Sputter Coater S 150 B), and viewed in a scanning electron microscope (LEO 420, Leo, Oberkochen, Germany).

Statistical analyses

All the following statistical tests were performed with log-transformed data. Before this transformation, the square root of the number of tarsal setae and the cube root of body mass were calculated. Simple linear regression analysis was used to test for the dependence of the maximal exerted pulling force on the number of tenent setae. The numbers of tarsal tenent setae were obtained from a previous publication (see table 1 in Betz, 2002), in which the tenent setae of each species were counted on the hind tarsi of five males and five females. To correct for body size, two separate linear regression analyses of both these log-transformed variables against log-transformed body mass were performed. The non-standardized residuals of these analyses (i.e. the difference between the data and a linear regression fitted to them) were then used to test for the final relationship between the two variables. The Tukey test was used to test for differences between the slopes of the different regression lines (Zar, 1999). Mann–Whitney *U*-tests were performed with the non-standardized residuals to test for overall differences in maximum pulling force between the group of species with slender tarsi (subgenera *Stenus* s. str. + *Nestus*) and the group of species with wide tarsi (subgenera *Hypostenus*, *Metastenus* and *Hemistenus*) on each of the various surfaces. To test for differences between the climbing performance of the same individuals on the different test surfaces, a Friedman test was performed, followed by the Wilcoxon test for paired comparisons (Sokal and Rohlf, 1995). The Wilcoxon test was also used to perform within-species comparisons of the climbing performance of individuals before

and after manipulation of the claws and the tenent setae. Interspecific comparisons of pulling forces were performed with pairwise Mann–Whitney *U*-tests. The significance levels of all the non-parametric pairwise tests that included more than one comparison were corrected according to the sequential Bonferroni procedure (Sokal and Rohlf, 1995). All statistical analyses were performed with SPSS 6.1. (SPSS Inc., Chicago, USA).

Results
Surface characteristics of the test surfaces

The selected surfaces are distinct with respect to both their surface roughness (Figs 2, 3) and their apparent surface energies and polarities (Table 1).

Surface roughness

Whereas glass represents an evenly smooth surface (Fig. 2A), the selected type of photographic paper has a uniformly roughened surface structure at the micrometre level (Fig. 2B). The surface of fresh *Glyceria* plants is smooth (similar to glass), but regularly interrupted by protruding longitudinal leaf veins (Fig. 2C). Protruding hairs or wax blooms are not present. In *Phragmites* leaves, the surface on and between the protruding leaf veins bears an array of tiny spines (Fig. 2D,E) and wax blooms (Fig. 2G). Dry *Phragmites* leaves (Fig. 2E) differ from fresh ones (Fig. 2D) by their significantly increased surface topography, indicated by distinct clefts and ridges. Filter paper represents a coarse network of thick fibres (Fig. 2F). The quantitative differences in surface roughness between the four test surfaces used in experiment 1 are shown in Fig. 3. As indicated by the illustrated surface profiles and *Ra* values, the surface roughness of the test surfaces increases in the order glass, photographic paper, dry *Phragmites* leaves and filter paper.

Table 1. *Measured advancing contact angles and calculated surface energies for the majority of test surfaces on which the pulling forces of the beetles were measured*

	Glass	Photographic paper	Dry *Phragmites*	Fresh *Phragmites*	Fresh *Glyceria*
Contact angle with water (degrees)	37.3±0.1 (*N*=3)	47.2±0.3 (*N*=3)	127.9±0.6 (*N*=4)	132.4±7.1 (*N*=3)	136.3±1.6 (*N*=3)
Contact angle with di-iodomethane (degrees)	59.3±0.1 (*N*=3)	55.6±0.7 (*N*=3)	104.5±0.6 (*N*=4)	109.1±2.5 (*N*=3)	111.0±1.9 (*N*=3)
Total surface energy (mN m^{-1})*	58.13	51.32	7.14	5.87	5.32
Polar component (mN m^{-1})	42.46	32.42	0.08	0.12	0.01
Dispersive component (mN m^{-1})	15.66	18.90	7.06	5.75	5.31
Surface polarity (%)[†]	70.04	63.17	1.12	2.09	0.19

The values of the contact angles are means ± S.D. *N* is number of samples measured.

For each sample, 35–52 single measured values were recorded automatically.

*Since the surface energies of natural solids are always composed of both energy and texture contributions, the calculated surface energies must not be considered as absolute values, which can only be determined for perfectly smooth surfaces.

[†]Calculated as (polar component of surface energy/dispersive component of surface energy)×100.
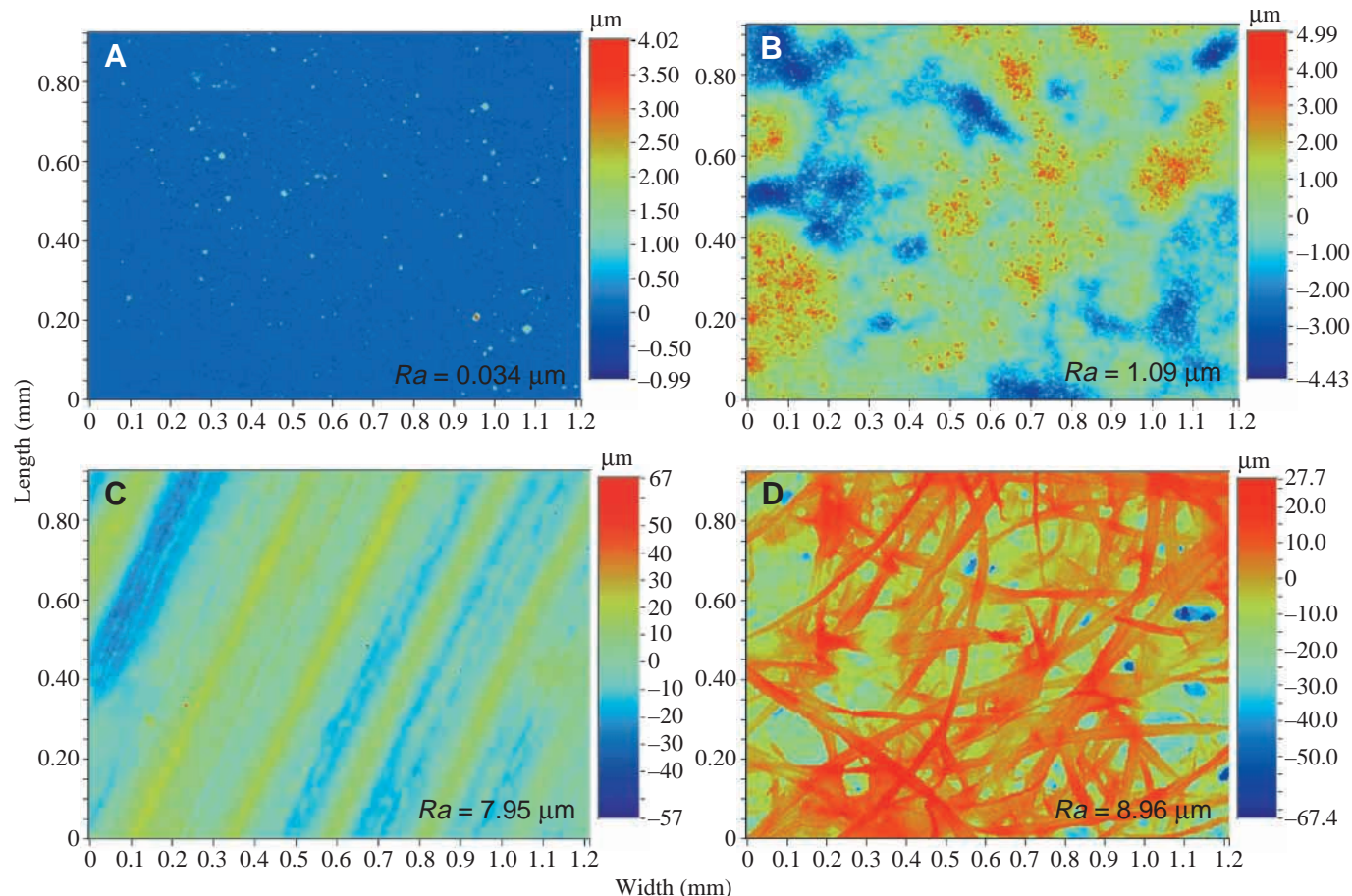
Fig. 3. Two-dimensional colour plots of the surface profiles of the test surfaces used in experiment 1. The plots were obtained using an optical surface profiler. The surface topographies can be inferred from the colour profiles and the *Ra* values (i.e. the means of the profile ordinates). Values of *Ra* (arithmetic means ± S.D.; *N*=3) are as follows: (A) glass microscope slide (*Ra*=0.034±0.002 μm), (B) photographic paper (*Ra*=1.09±0.2 μm), (C) dry leaf of *Phragmites communis* (*Ra*=7.95±0.4 μm) and (D) filter paper (*Ra*=8.96±0.6 μm). The dimensions (length and width) of the measured surface areas can be read off the *x*- and *y*-axes.

Surface energies and polarities

The apparent surface energies and polarities of the test surfaces, as calculated from the contact angle measurements, are summarized in Table 1.

Vertical climbing performance on a variety of surfaces

The absolute maximum pulling forces achieved by the beetles on various surfaces are summarized in Table 2. The pulling force to body weight ratios for the various surfaces are illustrated in Fig. 4. In general, the pulling forces in the species investigated increased in the order photographic paper, glass, dry *Phragmites* leaves, filter paper (Fig. 4; graphs on the left). The overall comparison of the body-weight-corrected pulling forces revealed that, on all four test surfaces, species with wide tarsi (subgenera *Hypostenus*, *Metastenus* and *Hemistenus*) on average exhibited significantly higher forces than species with slender tarsi (subgenera *Stenus* s. str., *Nestus*) (Mann–Whitney *U*-tests; significance levels on photographic paper and glass, *P*<0.001; on dry *Phragmites* leaves and filter paper, *P*≤0.05). However,

a clear distinction between the two groups was observed only on glass and on photographic paper (although, on the latter, three species with wide tarsi attained only relatively low pulling forces; see Fig. 4A). On both the other surfaces, single species with slender tarsi also accomplished high relative pulling forces and *vice versa* (Fig. 4; plots on the left). As indicated by the values of both the coefficient of determination (r^2) and the slope (*b*), the importance of the number of ventral tarsal tenent setae for the attained pulling forces is greatest on glass and decreases in the order photographic paper, dry *Phragmites* leaves and filter paper (Fig. 4; plots on the right). The slopes of the regression lines are similar for photographic paper and dry *Phragmites* leaves only; they are significantly different for all the other possible comparisons (pair-wise Tukey tests, *P*<0.05).

Relative significance of tarsal claws versus tenent setae for vertical climbing on a variety of surfaces

The results of the pulling force experiments conducted with manipulated animals are summarized in Table 3 (original

Table 2. *Maximum vertical pulling forces achieved by representatives of 18* Stenus *and one* Dianous *species on various substrata*

Species	N	Body mass (mg)	Vertical pulling forces on various surfaces (mN) (force/weight ratios are given in parentheses)			
			Glass	Photographic paper	Dry *Phragmites* leaves	Filter paper
sg. *Stenus* s. str.						
S. biguttatus L.	10	1.977±0.20	0.047±0.02[a] (2.4)	0.100±0.05[b] (5.3)	1.135±0.27[c] (58.5)	1.931±0.42[d] (101.0)
S. bimaculatus Gyllenhal	10	4.916±0.71	0.050±0.01[a] (1.1)	0.052±0.04[a] (1.2)	0.846±0.50[b] (18.2)	2.241±0.55[c] (45.9)
S. comma Leconte	10	2.617±0.31	0.092±0.06[a] (3.8)	0.106±0.04[a] (4.2)	0.949±0.19[b] (36.5)	1.823±0.25[c] (72.9)
S. fossulatus Erichson	10	1.926±0.29	0.145±0.08[a] (7.7)	0.120±0.05[a] (6.5)	0.750±0.20[b] (40.7)	1.536±0.29[c] (83.6)
S. juno Paykull	10	3.537±0.56	0.047±0.02[a] (1.4)	0.037±0.02[a] (1.1)	0.523±0.36[b] (15.7)	1.898±0.49[c] (56.6)
S. providus Erichson	3	2.439±0.16	0.081±0.06 (3.3)	0.055±0.03 (2.3)	0.381±0.11 (15.8)	1.511±1.02 (62.1)
sg. *Nestus*						
S. boops Ljungh	10	1.238±0.15	0.123±0.05[a] (10.0)	0.066±0.04[b] (5.6)	0.916±0.18[c] (75.8)	2.165±0.56[d] (177.3)
S. canaliculatus Gyllenhal	10	1.024±0.15	0.099±0.06[a] (10.3)	0.076±0.05[a] (8.3)	0.568±0.14[b] (57.8)	1.795±0.29[c] (178.5)
sg. *Hypostenus*						
S. cicindeloides Schaller	10	3.464±0.25	1.370±0.24[a] (41.0)	0.179±0.11[b] (5.2)	1.871±0.23[c] (54.9)	2.941±0.46[d] (85.6)
S. similis Herbst	10	2.942±0.27	0.970±0.28[a] (33.5)	0.424±0.22[b] (14.7)	0.875±0.18[a] (31.3)	2.321±0.28[c] (79.9)
S. solutus Erichson	10	2.782±0.25	1.551±0.33[a] (57.5)	0.596±0.25[b] (22.6)	1.419±0.51[a] (51.7)	2.756±0.70[c] (102.5)
S. latifrons Erichson	10	0.938±0.10	0.455±0.11[a] (50.2)	0.173±0.11[b] (18.8)	0.507±0.16[a] (55.2)	1.477±0.41[c] (159.8)
S. tarsalis Ljungh	10	1.592±0.16	1.223±0.14[a] (80.8)	0.400±0.14[b] (26.7)	1.269±0.45[a] (78.2)	2.195±0.36[c] (139.3)
sg. *Metastenus*						
S. bifoveolatus Gyllenhal	10	1.370±0.12	1.267±0.35[a] (94.5)	0.214±0.13[b] (16.0)	1.202±0.22[a] (93.3)	3.015±0.76[c] (220.7)
S. binotatus Ljungh	10	2.060±0.19	0.959±0.30[a] (49.5)	0.697±0.38[a] (34.4)	1.539± 0.41[b] (75.7)	2.622±0.97[c] (129.2)
S. nitidiusculus Stephens	10	2.196±0.18	1.355±0.19[a] (64.0)	0.173±0.11[b] (8.3)	1.648±0.29[c] (76.9)	3.253±0.72[d] (149.3)
S. pubescens Stephens	12	3.958±0.29	1.458±0.38[a] (38.7)	0.617±0.26[b] (16.4)	1.738±0.41[c] (44.7)	2.671±0.38[d] (66.7)
sg. *Hemistenus*						
S. impressus Germar	10	1.461±0.20	0.373±0.17[a] (25.5)	0.093±0.05[b] (6.4)	0.838±0.31[c] (62.6)	1.297±0.35[d] (90.6)
g. *Dianous*						
D. coerulescens Gyllenhal	10	3.899±0.44	0.169±0.09[a] (4.6)	0.120±0.04[a] (3.1)	1.635±0.26[b] (43.1)	2.856±0.35[c] (75.0)

Values are arithmetic means ± s.d.

Different letters refer to statistically significant intraspecific differences at the 5 % level (Friedman test, Wilcoxon test).

For *S. providus*, no statistical comparisons were performed because the sample size was too low.

For comparative purposes, the ratio of pulling force to body weight is added in parentheses.

The number of tarsal tenent setae for each species is listed in Table 1 of Betz (2002). The assignment of the species to subgenera follows Herman (2001). g, genus; sg, subgenus.
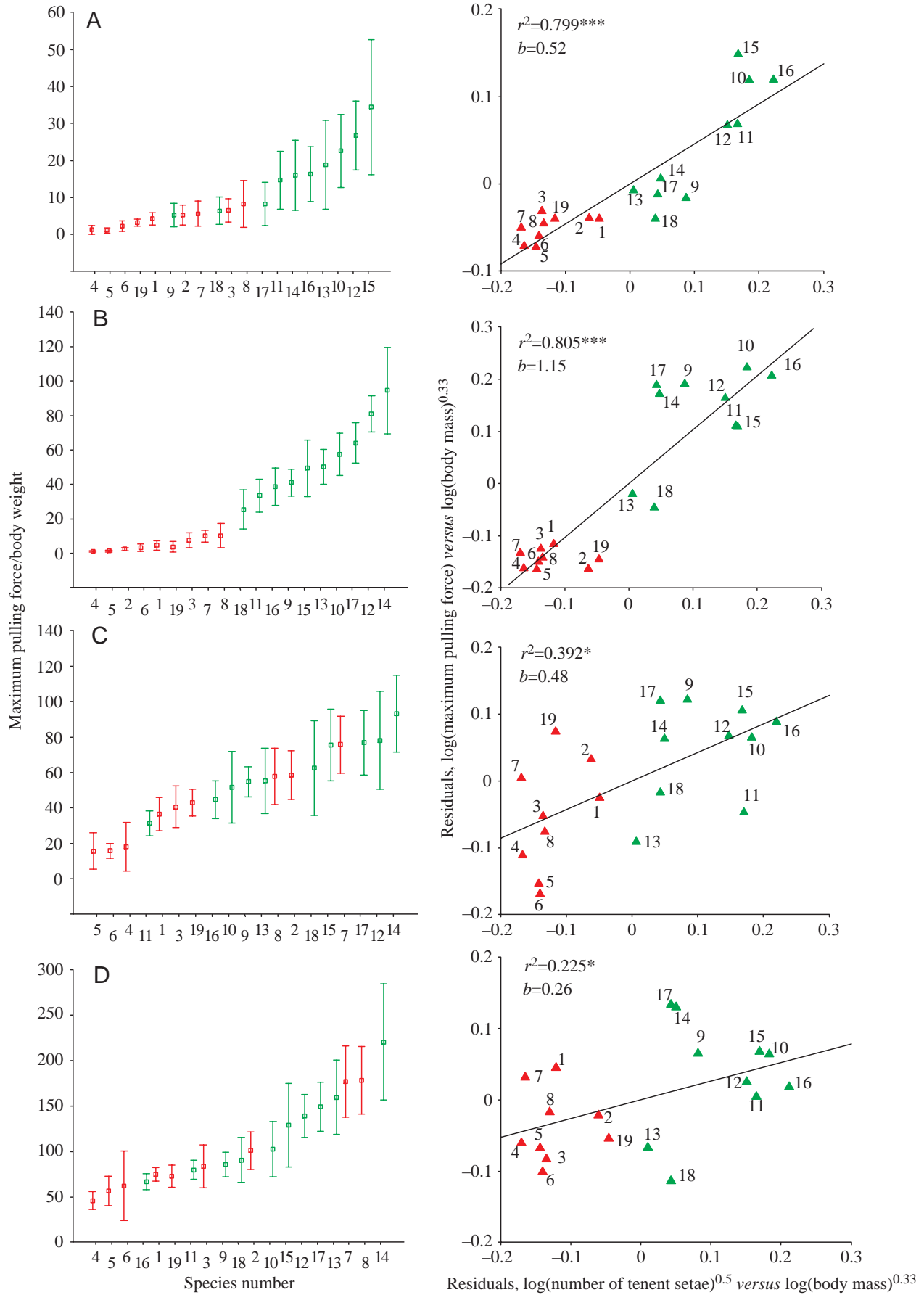
Fig. 4. Left: plots of maximum vertical pulling forces per body weight as achieved by representatives of 18 *Stenus* and one *Dianous* species on various surfaces (species-specific arithmetic means ± S.D.). Note the considerably higher pulling forces on filter paper (D). For sample sizes, see Table 2. Right: mean maximum vertical pulling forces as a function of the mean number of tarsal tenent setae, i.e. the number of tenent setae on one hind tarsus as reported in table 1 in Betz (2002). Before the analyses, both variables were corrected for body mass, as described in the text. (A) photographic paper, (B) glass slide, (C) dry *Phragmites* leaf, (D) filter paper. Red represents species with slender tarsi (subgenera *Stenus* s. str., *Nestus*), whereas green represents species with wide tarsi (subgenera *Hypostenus*, *Metastenus* and *Hemistenus*). Asterisks beside the coefficient of determination r^2 indicate different significant levels of the regression analysis: *$P \leqslant 0.05$; ***$P \leqslant 0.001$. *b*, slope. 1, *Stenus comma*; 2, *S. biguttatus*; 3, *S. fossulatus*; 4, *S. bimaculatus*; 5, *S. juno*; 6, *S. providus*; 7, *S. boops*; 8, *S. canaliculatus*; 9, *S. cicindeloides*; 10, *S. solutus*; 11, *S. similis*; 12, *S. tarsalis*; 13, *S. latifrons;* 14, *S. bifoveolatus*; 15, *S. binotatus*; 16, *S. pubescens*; 17, *S. nitidiusculus*; 18, *S. impressus*; 19, *Dianous coerulescens.*

Table 3. *Maximum vertical pulling forces achieved by representatives of three* Stenus *species on various substrata*

	Maximum vertical pulling force (mN)		
	S. comma	*S. pubescens*	*S. cicindeloides*
Intact tarsi (N=20)			
Glass	0.092±0.07	1.369±0.37	1.207±0.36
Fresh *Glyceria*	0.210±0.13	1.659±0.39	–
Fresh *Phragmites*	0.455±0.18	1.323±0.46	–
Dry *Phragmites*	1.071±0.19	1.236±0.27	1.171±0.31
Filter paper	1.880±0.35	3.024±0.36	2.824±0.78
Claws removed (N=10)			
Glass	0.070±0.04	1.350±0.35	1.153±0.40
Fresh *Glyceria*	0.079±0.04	1.551±0.30	–
Fresh *Phragmites*	0.086±0.06	1.049±0.34	–
Dry *Phragmites*	0.044±0.04	0.267±0.12	0.166±0.05
Filter paper	0.073±0.07	0.660±0.34	0.517±0.09
Neutralized tenent setae (N=10)			
Glass	0.034±0.02	0.047±0.02	0.076±0.05
Fresh *Glyceria*	0.092±0.04	0.106±0.03	–
Fresh *Phragmites*	0.223±0.11	0.210±0.07	–
Dry *Phragmites*	0.382±0.28	0.469±0.17	0.601±0.33
Filter paper	1.456±0.39	1.751±0.50	2.476±0.72

Values are arithmetic means ± S.D.
S. comma has slender tarsi; the other two species have wide tarsi.
–, not measured.

data) and Fig. 5 (corrected for body weight), which compare the performance of *S. comma* with slender tarsi with those of *S. pubescens* and *S. cicindeloides*, both of which have wide tarsi.

Stenus comma

In this species (Fig. 5A), the pulling forces per body weight on the smooth glass and fresh *Glyceria* leaf surfaces were very low even in intact beetles, so neutralization of the tenent setae had little effect. A considerable decrease in the pulling forces after the loss of the tenent setae was established on the dry *Phragmites* leaves only (on fresh *Phragmites* leaves, this decrease was much smaller, although statistically equally significant), whereas this decrease was trivial and statistically not significant on filter paper. Claw amputation resulted in a marked decline in the attainable pulling forces on all test surfaces that showed at least some degree of surface roughness (i.e. all the tested surfaces except glass).

Stenus pubescens

On the smooth glass and fresh leaf surfaces, intact beetles attained considerably higher pulling forces per body weight than *S. comma* (Fig. 5B). However, on the rougher surfaces of dry *Phragmites* and filter paper, the pulling forces were similar to those of *S. comma*. Neutralization of tenent setae reduced the pulling forces most drastically on the smooth glass and plant surfaces; this decline was more moderate on filter paper, although statistically equally significant. Removal of the claws had no effect on the pulling forces on the smooth glass and *Glyceria* surfaces. However, with increasing roughness of the test surfaces, the effect of claw removal became much more significant.

Stenus cicindeloides

This species (Fig. 5C) was only tested on three different surfaces and showed almost the same results as *S. pubescens*.

Significance of the specific structure of tenent setae

The pulling force experiments conducted with animals whose claws had been removed made it possible to estimate the significance of the size and specific structure of the single tenent setae by dividing the maximal attained pulling forces by the number of tenent setae and comparing this variable among species (Fig. 6). The species-specific numbers of tarsal tenent setae were obtained from counts performed by Betz (2002). It can be seen that, on the majority of test surfaces, the tarsal tenent setae of both the species with wide tarsi (*S. pubescens* and *S. cicindeloides*) allow significantly higher pulling forces than those of the species with slender tarsi (*S. comma*). The only instance when the pulling forces of individual tenent setae are almost identical between species with wide and slender tarsi is on dry *Phragmites* leaves (Fig. 6).

Wettability of the tarsi during locomotion on the surface of water

Videography of beetles of various species walking on the clean surface of tap water in a test container revealed that both species with wide tarsi and species with slender tarsi were supported by the surface film. While being supported, the beetles occasionally bent the apex of the abdomen downwards so that it came into contact with the water surface and thus supported the body, in addition to the legs (see Betz, 1999). When contacting the surface film, the bottom surface of the tarsi produced large roundish shadows surrounded by a bright halo. The centres of the shadows were sometimes
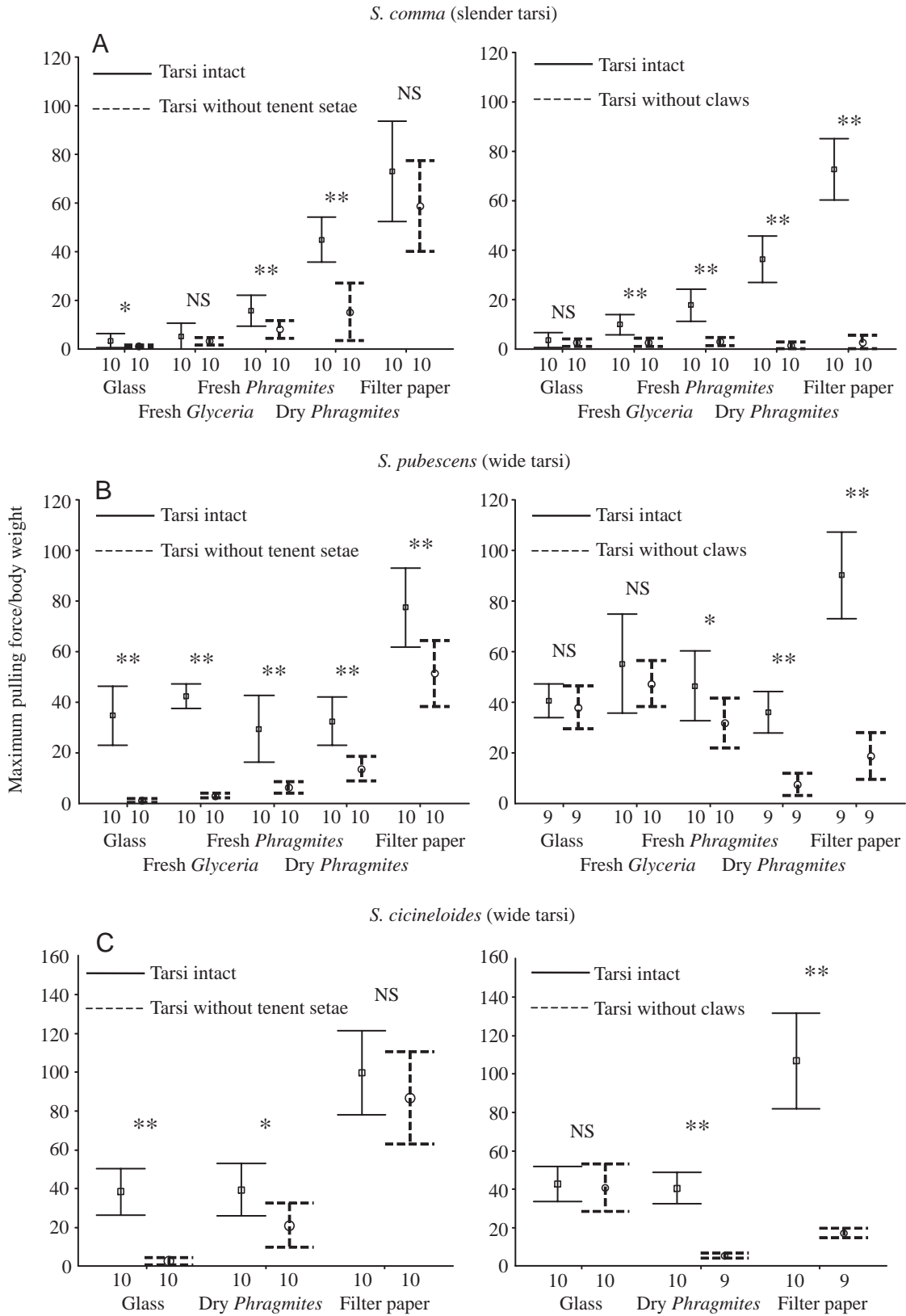
Fig. 5. Consequences of the 'neutralization' of tenent setae (plots on the left) and removal of the claws (plots on the right) on the attainable pulling forces (species-specific arithmetic means ± s.d.) on various surfaces in three different *Stenus* species with different tarsal morphologies: (A) *S. comma*, (B) *S. pubescens* and (C) *S. cicindeloides*. The test surfaces are arranged in order of increasing surface topography. The asterisks above the error bars refer to the significance levels of Wilcoxon tests for paired comparisons: *$P \leqslant 0.05$; **$P \leqslant 0.005$; NS, not significant. Values of N are given below the *x*-axes.
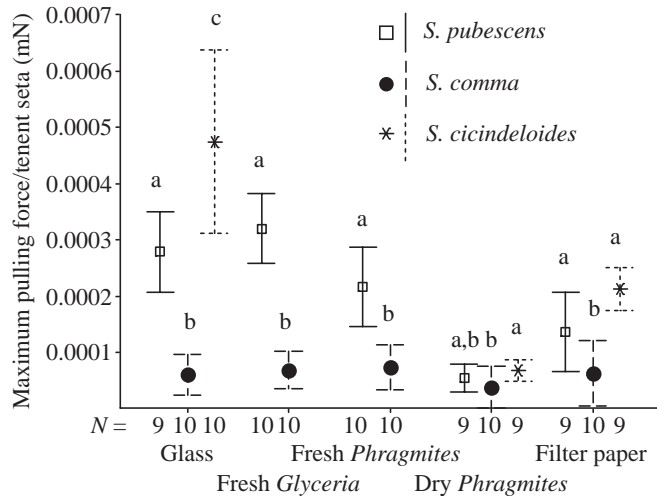
Fig. 6. Comparisons of pulling forces per single tenent seta between claw-amputated beetles of three *Stenus* species on various test surfaces (arithmetic means ± S.D.). Values of *N* are given below the *x*-axes. During maximum pulling performance, all six tarsi usually have contact with the test surface, so the maximum pulling forces were divided by the total number of tenent setae on all six tarsi. The latter was approximated by multiplying the number of tenent setae counted on the hind tarsi (see table 1 in Betz, 2002) by six. *S. pubescens* and *S. cicindeloides* are species with wide tarsi, whereas *S. comma* has slender tarsi. *S. cicindeloides* was tested on only three of the five surfaces. The letters above the error bars indicate statistically significant interspecific differences (Mann–Whitney *U*-test; *P*<0.05).

superimposed by one sharp luminous point (Fig. 7). The measured apparent contact angles between the bottom surface of the tarsi of the various species and water together with the other variables necessary to calculate the forces supporting the beetles on the surface film are given in Table 4. It can be seen that, from a theoretical point of view, both tarsal morphologies permit sufficient support by the surface of water (safety coefficients >1), which is mainly attributable to the high apparent contact angles between the ventral sides of the tarsi and the water (Table 4). The effect of buoyancy on supporting the beetles on the surface of water is negligible in all the species examined (Table 4).

Discussion

The present study is an experimental approach to evaluating the biological role of widened bilobed tarsi, which have evolved in various lineages within the staphylinid genus *Stenus*. Reliable phylogenies at the species level are not yet available for this genus. However, there is good evidence that the subgenera *Stenus* s. str. plus *Nestus* form a monophylum comprising species with slender weakly or non-bilobed tarsi. According to outgroup comparisons, this state represents the phylogenetically antecedent condition compared with the wide distinctly bilobed tarsi (V. Puthz, personal communication), which might have evolved several times independently in the subgenera *Hypostenus*, *Metastenus* and *Hemistenus*.

Fig. 7. Video frame of a *Dianous coerulescens* walking on the surface of water in a test chamber illuminated obliquely from above. Note the ovoid shadows on the ground produced by the tarsi and the superimposed luminous points presumably produced by the claws. The length of the beetle is approximately 6 mm.

I have evaluated tarsal performance under two different potential selective regimes: locomotion on a surface film and climbing up vertical structures. The use of widened tarsi in contexts such as copulation can be ruled out, because (i) in the vast majority of *Stenus* species, there are no obvious sex-specific differences in tarsal morphology, (ii) the tarsi are widened not only in the forelegs but also in the middle- and hindlegs, and (iii) species in lineages with widened tarsi copulate in an end-to-end position, which does not require the male to grasp the female. However, several species with slender tarsi mate only in a parallel position (Betz, 1999), a position in which widened tarsi in the male would indeed be more advantageous. In the following, I consider the usefulness of widened tarsi *versus* slender tarsi in *Stenus* and in one *Dianous* species in the context of locomotion on the surface of water and vertical climbing on various surface textures. Finally, I discuss the contribution of my results to our understanding of the mechanism of insect tarsal attachment to differently textured solids.

The role of tarsal morphology during walking on the surface of water

Many representatives of the Steninae live in damp environments, where they can be found running on the ground or climbing on a variety of plants. In these habitats, the beetles need to be able to cross patches of free surface water and, indeed, three different modes of locomotion can be distinguished on a surface film (Betz, 1999): (i) walking on the surface film as if it were firm ground, following the same mode of leg coordination as during terrestrial locomotion, (ii) swimming, while the tarsi, tibiae and the entire undersurface of the body make contact with the surface of the water and perform typical swimming movements without becoming

Table 4. *Support of selected similar-sized species with slender tarsi versus those with wide tarsi by the surface of water*

	Species with slender tarsi					Species with wide tarsi		
	Dianous coerulescens	*Stenus comma*	*S. fossulatus*	*S. juno*	*S. providus*	*S. similis*	*S. solutus*	*S. pubescens*
Mean body weight (N) (N=10–12)	$3.83\times10^{-5}\pm4.1\times10^{-6}$	$2.57\times10^{-5}\pm3.0\times10^{-6}$	$1.89\times10^{-5}\pm2.7\times10^{-6}$	$3.47\times10^{-5}\pm5.3\times10^{-6}$	$2.39\times10^{-5}\pm1.3\times10^{-6}$	$2.88\times10^{-5}\pm2.6\times10^{-6}$	$2.73\times10^{-5}\pm2.4\times10^{-6}$	$3.88\times10^{-5}\pm2.9\times10^{-6}$
Mean hind tarsus width (m) (N=10)	$8.00\times10^{-5}\pm1.2\times10^{-6}$	$4.94\times10^{-5}\pm1.5\times10^{-6}$	$4.06\times10^{-5}\pm7.3\times10^{-7}$	$4.98\times10^{-5}\pm1.0\times10^{-6}$	$4.62\times10^{-5}\pm1.3\times10^{-6}$	$1.10\times10^{-4}\pm2.3\times10^{-6}$	$1.11\times10^{-4}\pm2.0\times10^{-6}$	$1.30\times10^{-4}\pm1.9\times10^{-6}$
Mean tarsus length[a] (m) (N=10)	$7.44\times10^{-4}\pm2.6\times10^{-5}$	$7.75\times10^{-4}\pm1.7\times10^{-5}$	$6.22\times10^{-4}\pm1.8\times10^{-5}$	$6.73\times10^{-4}\pm3.3\times10^{-5}$	$6.43\times10^{-4}\pm2.7\times10^{-5}$	$5.88\times10^{-4}\pm2.0\times10^{-5}$	$5.54\times10^{-4}\pm1.9\times10^{-5}$	$5.61\times10^{-4}\pm2.8\times10^{-5}$
Mean apparent contact angle between tarsal ventral surface and water (degrees)	147.30 ± 2.2 (N=4)	138.58 ± 7.5 (N=5)	101.77 ± 4.9 (N=4)	138.74 ± 9.4 (N=7)	138.61 ± 11.5 (N=4)	150.85 ± 8.7 (N=6)	148.48 ± 4.1 (N=4)	149.16 ± 4.6 (N=4)
Line of contact of tarsal ventral surface with water (m)	1.65×10^{-3}	1.65×10^{-3}	1.33×10^{-3}	1.45×10^{-3}	1.38×10^{-3}	1.40×10^{-3}	1.33×10^{-3}	1.38×10^{-3}
Buoyancy (N)	3.67×10^{-11}	1.46×10^{-11}	7.86×10^{-12}	1.29×10^{-11}	1.05×10^{-11}	4.81×10^{-11}	5.26×10^{-11}	7.30×10^{-11}
Vertical component of surface tension (N)	9.50×10^{-5}	8.40×10^{-5}	1.85×10^{-5}	7.43×10^{-5}	7.10×10^{-5}	8.37×10^{-5}	7.77×10^{-5}	8.10×10^{-5}
Safety coefficient	7.44	9.81	2.93	6.42	8.91	8.71	8.53	6.26

The calculations were performed according to equations 1–5 in Materials and methods.

Body parameters necessary for the calculations are also listed.

Further assumptions: surface tension of water=0.0685 N m^{-1} (=mean of both the measurements reported in the Materials and methods section); density of water 1 kg m^{-3}.

[a]Calculated as the average of fore, middle and hind tarsus length.

Values are arithmetic means ± S.D.

immersed, and (iii) expansion skating, i.e. rapidly skimming over the surface film by releasing an abdominal secretion (see Jenkins, 1960; Linsenmair, 1963).

The function of the tarsi is most critical during normal walking on the surface film since, in this case, the bottom surfaces of the tarsi form the only interfaces with the water, sometimes supported by the ventrally bent apex of the abdomen. As shown in Fig. 7, the tarsi of the Steninae walking on the surface film in a test container produce large shadows surrounded by bright halos, indicating their non-wettability (see Baudoin, 1976). However, a single luminous point can also be seen within these shadows; this must be produced by some wettable structure on the tarsi. As in semiaquatic bugs (Baudoin, 1976; Darnhofer-Demar, 1969; Møller Andersen, 1976), these luminous points are probably caused by the smooth, and thus more-wettable, claws penetrating the surface film.

The contact angle measurements confirm that the investigated Steninae have especially water-repellent tarsal ventral surfaces with apparent contact angles with water of up to 150° (Table 4). Contact angles of this size cannot be achieved by the hydrophobic chemical composition of the cuticle surface alone, but only by additional surface roughness (e.g. Crisp, 1963; Holdgate, 1955; Noble-Nesbitt, 1963). In contrast to smooth tarsal attachment systems such as euplantulae and arolia, tarsi with an array of obliquely inclined ventral tenent setae have the potential to form this roughness, causing an increase in water-repellency as required for safely supporting a walking insect on the surface film. However, this is achievable only when the tarsal tenent setae are impregnated with a hydrophobic lipid layer, increasing the true contact angle beyond 90° (e.g. Holdgate, 1955).

In several *Stenus* species, it has been demonstrated that the beetles release a secretion through their tarsal tenent setae; the lipid component of this secretion resembles the composition of the superficial lipid coating of the body surface (Betz, 2002). Since the lipid fraction is mainly a mixture of unsaturated fatty acid glycerides and aliphatic hydrocarbons, i.e. neutral lipids, it should have little tendency to spread over a water surface. Hence, it can be assumed that high contact angles on the bottom of the tarsi can be maintained, even after prolonged contact with water, by the subsequent delivery of a hydrophobic secretion, which is distributed over the tarsi and the other parts of the body surface by intense self-grooming. Grooming has been observed to take up 5–50% of the time budget in *Stenus* species (Betz, 1999), underlining its biological significance. When submerged, the tarsi and other parts of the body have

a silvery appearance, provided by air entrapped between the unwettable hairs. Such air films are well known from other semi-aquatic insects, such as water striders (e.g. Crisp, 1963), and are responsible for the considerable increase in the apparent contact angle beyond the true contact angle (Adam, 1963).

The contact angle measurements performed on the bottom surface of the tarsi demonstrate that, in all the species examined, the tarsi, irrespective of whether they are wide or slender, provide adequate safety coefficients to support the beetles on the surface of water (Table 4). These values are sufficient to support the body on the surface film, even if the surface energy of the water is reduced by natural surfactants. As can be deduced from Table 4, species with slender tarsi nevertheless attain considerable perimeters of the line of contact between the tarsus and the water surface because their small tarsal width is more than compensated for by their increased tarsal length. Consequently, their safety coefficients are not necessarily lower than those of species with widened tarsi. According to these results, it can be concluded that there have been no selective demands in this biological context to drive the widening of the tarsi within the Steninae. The actual safety coefficients for all the species examined must be considered to be even higher, because the method used to calculate buoyancy (equation 5 in Materials and methods) somewhat underestimates the upward force exerted by the water surface; the calculated buoyancy only considers that of the tarsus itself, whereas the depression in the surface film caused by the tarsus has a volume that must be considered as being larger than that of the tarsus (see Suter et al., 1997; Suter and Wildman, 1999). According to these authors, such depressions associated with leg/surface-film contact are employed by many water-walking organisms to produce the horizontal thrust necessary for propelling themselves over the surface film.

The role of tarsal morphology during climbing on a variety of surfaces

As in other studies of insect tarsal attachment using strain-gauge force transducers (e.g. Dixon et al., 1990; Lees and Hardie, 1988; Stork, 1980a; Walker et al., 1985), the present study considers vertical pulling forces exerted by tethered animals as indicators of tarsal attachment performance. The advantage of this method is that the animals can be directly observed during the experiments, ensuring that they actually exert their maximum performance abilities. While doing so, the Steninae beetles usually attach to the surface with all six tarsi simultaneously.

In an initial experiment, the attachment performance of beetles of 19 species was tested on four different surfaces (Fig. 4). This experiment revealed that widened tarsi associated with considerably more tenent setae had significantly higher attachment capacities. The presence of a large number of tarsal tenent setae was also of marked significance on smooth plant surfaces such as *Glyceria maxima*, as used in the second experiment with manipulated beetles (Fig. 5). On surfaces with increased roughness, the importance of the number of tarsal tenent setae decreased, some species with slender tarsi also attaining relatively high pulling forces (Fig. 4). This indicates that, on these surfaces, the claws become functionally more important, since they enable the beetles to cling to protruding elements of the surface and subsequently to use this firm anchoring point to draw up the rest of the body.

To elucidate the relative significance of the tarsal tenent setae *versus* that of the pretarsal claws, a second series of experiments was undertaken, which allowed a comparison of the attachment performance of beetles before and after neutralization of the tarsal tenent setae and the claws (Fig. 5). This experiment clearly demonstrated the significance of the widened bilobed tarsi on smooth surfaces such as glass or fresh *Glyceria* leaves: whereas *S. comma* beetles with slender tarsi did not attain large pulling forces on these surfaces either with intact tarsi or with neutralized tenent setae (Fig. 5A), the neutralization of the tenent setae greatly diminished the attachment performance of both species with wide tarsi (*S. pubescens* and *S. cicindeloides*) (Fig. 5B,C). At the same time, claw removal, but with intact tenent setae, did not affect movement on these smooth surfaces. In contrast to the conditions on these smooth surfaces, the tenent setae are of minor importance on very rough surfaces, here exemplified by filter paper. On this surface, claw removal reduced attachment capabilities drastically in all the test species irrespective of their tarsal morphologies, whereas the effect of the neutralization of the tenent setae was much smaller (Fig. 5).

The results attained on both dry and fresh *Phragmites* surfaces are of special interest since the characteristics of smooth and rough surfaces appear to be united in both these surfaces. This is indicated by the observation that, in all the three test species irrespective of their tarsal morphology, both the neutralization of the tenent setae and the amputation of the claws significantly reduce the attainable pulling forces (Fig. 5). Therefore, pretarsal claws and tarsal tenent setae are probably functionally linked on these surfaces and work synergistically. The possible mechanism behind this is discussed in more detail in the next section.

In *Stenus* species with especially widened tarsi, not only is the bottom surface of the tarsus provided with more tenent setae but the quality of the single tenent setae is also different. In the 19 species investigated, nine different morphological types of tarsal ventral setae could be identified (see figs 3 and 4 in Betz, 2002). Whereas the majority of these types probably have mechanoreceptive functions, three of them can be assigned as tenent setae. One of these types occurs in all the investigated species irrespective of their tarsal morphology. It is terminally tapered and sub-apically recurved, but otherwise shows no specific terminal differentiation (see figs 3c,d; 4a,e in Betz, 2002). However, species with widened tarsi have an additional type of tenent seta, which is distally spatulate (see figs 3h and 4c in Betz, 2002). Tenent setae of this type are also found among many other groups of beetles (Stork, 1980b) and can be assumed to develop higher adhesive forces as a result of their increased area of contact with the substratum.

The significance of the specific morphology of the tenent setae for attachment performance in *Stenus* beetles can be roughly assessed by comparing the maximum pulling forces divided by the total number of tenent setae among beetles whose claws were removed (Fig. 6). Indeed, these calculations show that, in addition to the number of tenent setae, their size and morphology are also of vital importance. On the vast majority of the test surfaces, the calculated pulling forces per tenent seta are higher in *S. pubescens* and *S. cicindeloides* compared with *S. comma* with its slender tarsi (Fig. 6). This is probably attributable to the sole-like enlarged apices that are present on the tenent setae in both the first two species and that might also be better supplied with adhesive secretion. These spatulate apices probably provide the setae with a larger area of contact with the substratum. The specific tarsal morphology is of no major importance if the beetles try to move on dry *Phragmites* leaves. The possible reason for this is discussed in the next section.

As shown above, the especially widened bilobed tarsi in *Stenus* beetles are not vital for supporting the beetles on the surface of water. Indeed, the results of the pulling force experiments suggest that the main selective demands have come from the attachment to smooth plant surfaces. The peak pulling forces in species with slender tarsi on smooth surfaces amount to 1–10 times their own body weights (cf. Table 2 and Table 3), but this is obviously not a sufficient safety factor to make possible the more permanent settlement of the vegetation. First, the listed pulling forces represent the maximum performance abilities only when the beetles attach themselves to the surface with all six tarsi. The exerted pulling forces are usually considerably lower (see Fig. 1), because during normal walking only three tarsi are simultaneously in contact with the surface and the attachment to the surface will not be always optimal. Second, wide tarsi might be not only important for mounting vertical structures but also for resisting horizontal detachment forces caused by the drag and whiplash of moving leaves. According to the projections of Stork (1980a) and assuming that leaves oscillate in a strong gusty wind in a harmonic motion, insects have to withstand detachment forces of approximately 16 times their body mass. As can be seen from Table 2 and Fig. 4, on smooth surfaces, such as glass or fresh leaves, only species with wide tarsi (subgenera *Hypostenus*, *Metastenus* and *Hemistenus*) attain pulling force/body weight ratios that clearly exceed this value, whereas those of species with slender tarsi (subgenera *Stenus* s. str., *Nestus*, and the one *Dianous* species examined) remain below this value.

The experimental results of the present study demonstrate the importance of wide tarsi, accommodating a large number of tarsal setae, for climbing on vertical plant surfaces. Recalling that, in *Stenus* beetles, slender weakly or non-bilobed tarsi most probably represent the phylogenetically antecedent condition compared with the wide distinctly bilobed tarsi, the evolution of wide tarsi in the various lineages might represent a key innovation that has made possible the expansion of the adaptive zone to live plants, contributing to the tremendous radiation of this genus. Indeed, approximately 70 % of the more than 2100 *Stenus* species described belong to three subgenera (*Hypostenus*, *Metastenus* and *Hemistenus*) whose representatives have wide bilobed tarsi (V. Puthz, personal communication). Unbalanced clade diversities of this order might justify consideration of the evolution of wide bilobed tarsi in *Stenus* as a key innovation. With reliable phylogenies available, this hypothesis might be testable in the future using statistical approaches (e.g. Bond and Opell, 1998).

Mechanisms of tarsal attachment to a variety of surfaces

The present study was conceived mainly to evaluate the adaptive value of various tarsal morphologies and it also contributes to our understanding of the general mechanism of tarsal attachment to different substrata. The test surfaces used in this study differ mainly (i) in their surface roughness (Figs 2–3), (ii) in their free surface energies and (iii) in their surface polarities (Table 1), which makes it possible to infer the relative functional roles of both the pretarsal claws and the tarsal tenent setae and the possible characteristics of the tarsal adhesive secretion from the performance data.

Rough surfaces

The mechanism of insect tarsal attachment to differently textured surfaces has been the subject of various previous studies (e.g. Dixon et al., 1990; Gorb et al., 2001; Jiao et al., 2000; Lees and Hardie, 1988; Roth and Willis, 1952; Stork, 1980a; Walker et al., 1985), some of them aiming at illuminating the relative significance of the pretarsal claws *versus* the tarsal tenent setae and the smooth attachment pads. Two of these studies have emphasized the predominant role of the claws on rough surfaces (Roth and Willis, 1952; Stork, 1980a). As discussed in the previous section, this view is in good agreement with the results of the present study. Hence, on rough surfaces, the maximally attainable pulling forces should be limited only by (i) the leverage and maximum power output of the leg muscles and (ii) the yielding strength of the pretarsus and the surface projections of the substratum. For the latter, the shape of the claws in relation to the surface topography (structure and magnitude) may be of special importance. However, even on filter paper, the tarsal tenent setae have a significant (although weak) supporting effect on the pulling forces exerted (Figs 4D, 5B), suggesting their mechanical interlocking with surface irregularities.

Smooth surfaces

The vertical pulling forces measured in this study represent attachment forces that work parallel (non-normal) to the plane of the surface at the interface between the tarsal tenent setae and the substratum. In insects, a tarsal secretion sandwiched between the ventral tarsus surface and the substratum is considered to be a vital component of attachment in both hairy and smooth systems (e.g. Jiao et al., 2000). This is especially true of smooth surfaces which, in the present study, are represented in various forms by the glass, photographic paper, fresh *Glyceria* leaves and, to a lesser degree, fresh *Phragmites*

leaves. The underlying attachment forces acting parallel to the substratum are generally considered to be a combination of capillary, viscous, friction and, at close contacts, molecular forces (e.g. Gorb and Scherge, 2000; Jiao et al., 2000; Scherge and Gorb, 2001; Wigglesworth, 1987).

As mentioned above, *Stenus* species with both slender and wide tarsi release a tarsal secretion *via* their tenent setae; this is visible as footprints on a glass surface. According to its neutral lipid content (Betz, 2002), this secretion has two functions: (i) to keep the ventral surface of the tarsi water-repellent (as discussed above) and (ii) to wet a variety of plant surfaces to improve attachment forces during locomotion. Despite their high surface polarities, surfaces such as glass and photographic paper have sufficiently high free surface energies to allow possible wetting by even apolar lipid secretions (Table 1) (see McFarlane and Tabor, 1950). In contrast, surface energies can be extremely low on waxy plant surfaces (Table 1) and might thus impede wetting by even non-polar lipid tarsal secretions.

However, the results showing that the pulling forces of claw-amputated beetles on fresh *Glyceria* and *Phragmites* leaves are similar to (or even larger than) those attained on glass (Table 3; Fig. 5) suggest that the tarsal secretion might be capable of spreading on even these extremely hydrophobic surfaces. This might be understandable under the two-component surface energy approach (e.g. Wu, 1973), according to which complete wetting of a low-energy substratum by a low-energy adhesive might be still possible on condition that the surface polarities of both the adhesive and the substratum match closely. Hence, insect tarsal secretions should generally be expected to be mixtures of neutral lipids with only low (if any) contents of polar components such as fatty acids, esters and alcohols. The few attempts to analyse the tarsal secretion of insects chemically support this hypothesis (e.g. Attygalle et al., 2000; Betz, 2002; Ishii, 1987; Kosaki and Yamaoka, 1996). The spread of such adhesives would be further facilitated by maintaining their viscosity as low as possible (McFarlane and Tabor, 1950; Zisman, 1964). The main contribution of the adhesive to attainable adhesion is presumably attributable to its viscosity rather than to its capillarity, because the pulling forces measured in this study are exerted parallel to the substratum (e.g. Denny, 1993; Jiao et al., 2000).

It has not as yet been possible to determine the thickness of the secretion sandwiched between the tarsal tenent setae and the substratum; this would be crucial for a quantitative assessment of the relative contribution of those forces to the observed pulling forces. However, for the adhesive pads of *Tettigonia viridissima*, it has recently been shown that the tarsal secretion does not completely account for the adhesive forces exerted vertical to the substratum (Jiao et al., 2000), so that additional friction and/or intermolecular forces are probably involved (see Persson, 1998).

Another interesting result of the present study is the low attachment of the tarsi to the photographic paper. This substratum yielded the lowest measured pulling forces of all the tested surfaces, especially in species with wide tarsi

(Table 2). Although its surface is actually uniformly roughened (Figs 2B, 3B), photographic paper is here treated as a smooth surface because its surface irregularities are obviously an order of magnitude too small (indicated by its low Ra value of 1.09) to present an opportunity for the claws to cling to it. This can be deduced from the finding that the pulling forces exerted on photographic paper are even lower than those attained on glass (Table 2), on which the claws have been shown not to contribute to the overall pulling force (Table 3; Fig. 5). Since the surface energies and polarities of the photographic paper are very similar to those of the glass (Table 1), the reduced attachment forces on photographic paper are not likely to be attributable to its lower wettability by the secretion. Rather, they must be considered to be the result of the reduced area of real contact between the roughened surface of the photographic paper and the tarsal tenent setae; this would substantially reduce attachment forces caused by both adhesion and friction (e.g. Persson, 1998; Scherge and Gorb, 2001). The same effect is probably responsible for the reduced attachment forces of claw-amputated beetles on dry *Phragmites* leaves compared with fresh ones (Table 3; Fig. 5), because wilting results in an increased surface corrugation (compare Fig. 2E with Fig. 2D). This takes place not only on a large-scale level, resulting in longitudinal semi-cylindrical ridges, but also at the level of the epidermis cells, forming distinct bulges (Fogg, 1947, 1948).

Surfaces that combine attributes of both rough and smooth surfaces

Many natural plant surfaces usually combine the surface characteristics of both rough and smooth substrata, because the smooth plant epidermis might be regularly disrupted by protuberances, such as cuticular folds, leaf veins, trichomes or wax crystalloids (e.g. Juniper and Jeffree, 1983). The wax crystalloids on glaucous plant surfaces might actually physically impede the adhesion of insect tarsi (i) by reducing the actual area of contact, (ii) by contaminating the tenent setae and (iii) by exfoliating as the insect walks on the surface (e.g. Brennan and Weinbaum, 2001; Eigenbrode, 1996; Juniper and Burras, 1962; Stork, 1980c). This effect is probably responsible for the reduced adhesion, especially of claw-amputated *Stenus* beetles, to *Phragmites* surfaces compared with *Glyceria* leaves (Table 3; Fig. 5) because protruding wax blooms have been detected on *Phragmites* leaves only (see Fig. 2G). Consequently, the specific structure of the single tenent setae is of no importance on the latter (see Fig. 6).

However, as indicated in the previous section, the claws are to some extent capable of making up this shortcoming, suggesting a hitherto overlooked functional synergism between claws and tarsal tenent setae. Since both the removal of the claws (leaving the tarsal tenent setae intact) and the neutralization of the tenent setae (leaving the claws intact) result in a significant decrease in the pulling forces, the claw function probably adds to the adhesion and friction force mediated by the tenent setae. This can be illustrated by a simple mechanical analogue in which the tarsus is considered as a
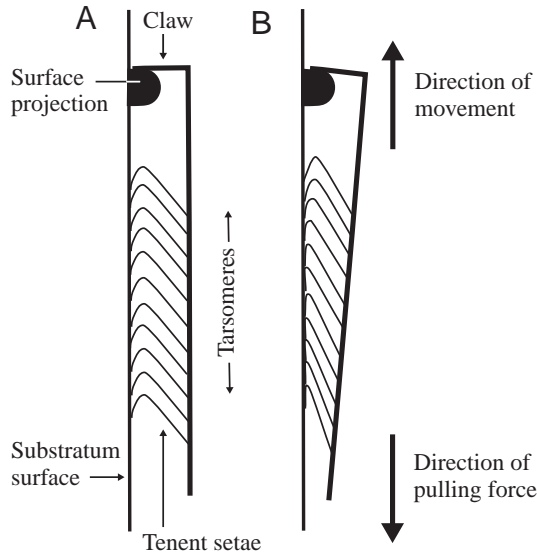
Fig. 8. Functional model illustrating the suggested synergistic behaviour of the claws and tarsal tenent setae during vertical upward climbing on plants that combine attributes of both rough and smooth surfaces. (A) First, the claws cling to a surface irregularity; (B) because of the downward-directed pull of the leg, the ventral sides of the tarsomeres are subsequently pressed against the substratum, compressing the tarsal tenent setae. Note that this model assumes sub-apically recurved setae, but is also valid for smoothly curved setae.

hook-like lever rotating about a projection or crevice of the substratum to which the claws cling (Fig. 8). During vertical upward climbing, this construction results in the tarsus being pressed against the surface, causing spring-like compression of the elastic tenent setae (Fig. 8B). Consequently, according to the counterforce exerted by the tenet setae, the load of the tarsus directed normal to the surface and, thereby, the real area of contact between the tarsus and the substratum are increased.

Such conditions would actually enhance the attachment forces according to both mechanisms of attachment considered, i.e. friction and adhesion, attributable to the viscosity of the secretion (e.g. Bowden, 1957; Persson, 1998; Scherge and Gorb, 2001). Whereas the first part of the mechanical analogue (i.e. clinging of the claws to a surface irregularity and subsequent pressing of the tarsus against the surface) has been directly observed in tethered beetles, the proposed spring-like behaviour of single tarsal tenent setae has not as yet been confirmed by direct observation but can be inferred from the internal setal flexibility and curved appearance. The increase in attachment forces acting parallel to the substratum with increasing normal loads has recently been empirically demonstrated in 'smooth' systems, such as the attachment pads of the locust *Tettigonia viridissima* (Jiao et al., 2000), and in 'hairy' systems as exemplified by gecko feet (Autumn et al., 2000). The latter study has shown that the parallel pulling forces attained by single gecko foot-hairs depend on the initial preload, which does not have to be maintained during subsequent pulls. Applied to the mechanical

analogue of Fig. 8, this means that, in insects that climb upwards on vertical surfaces, an initial grasp of the claws to some surface irregularity might suffice to increase significantly the subsequent attachment forces exerted by the tenent setae, even when the claws no longer cling to the surface. This would be especially important on plant surfaces with relatively weak and/or small surface projections, which (unlike filter paper) would easily give way under the subsequent stronger shear forces exerted by the claws.

References

Adam, N. K. (1963). Principles of water-repellency. In *Waterproofing and Water-Repellency* (ed. L. L. Moilliet), pp. 1–23. Amsterdam: Elsevier.

Anderson, R. (1984). Staphylinidae (Coleoptera) in Ireland. III. Steninae. *Ir. Nat. J.* **21**, 242–251.

Attygalle, A. B., Aneshansley, D. J., Meinwald, J. and Eisner, T. (2000). Defense by foot adhesion in a chrysomelid beetle (*Hemisphaerota cyanea*): characterization of the adhesive oil. *Zoology* **103**, 1–6.

Autumn, K., Liang, Y. A., Hsieh, S. T., Zesch, W., Chan, W. P., Kenny, T. W., Fearing, R. and Full, R. J. (2000). Adhesive force of a single gecko foot-hair. *Nature* **405**, 681–685.

Baudoin, R. (1976). Les insectes vivant à la surface et au sein des eaux. In *Traité de Zoologie*, Tome VIII, Fasc. IV (ed. P.-P. Grassé), pp. 843–926. Paris: Masson et Cie.

Betz, O. (1994). Der Fangapparat bei *Stenus* spp. (Coleoptera, Staphylinidae): Bau, Funktion, Evolution. Dissertation, Universität Bayreuth. 239pp.

Betz, O. (1996). Function and evolution of the adhesion-capture apparatus of *Stenus* species (Coleoptera, Staphylinidae). *Zoomorphology* **116**, 15–34.

Betz, O. (1998a). Comparative studies on the predatory behaviour of *Stenus* spp. (Coleoptera: Staphylinidae): the significance of its specialized labial apparatus. *J. Zool., Lond.* **244**, 527–544.

Betz, O. (1998b). Life forms and hunting behaviour of some Central European *Stenus* species (Coleoptera, Staphylinidae). *Appl. Soil Ecol.* **9**, 69–74.

Betz, O. (1999). A behavioural inventory of adult *Stenus* species (Coleoptera: Staphylinidae). *J. Nat. Hist.* **33**, 1691–1712.

Betz, O. (2002). Structure of the tarsi in some *Stenus* species (Coleoptera, Staphylinidae): External morphology, ultrastructure and tarsal secretion. *J. Morphol.* (in press).

Bock, W. J. (1988). The nature of explanations in morphology. *Am. Zool.* **28**, 205–215.

Bock, W. J. (1990). From Biologische Anatomie to ecomorphology. *Neth. J. Zool.* **40**, 254–277.

Bond, J. E. and Opell, B. D. (1998). Testing adaptive radiation and key innovation hypotheses in spiders. *Evolution* **52**, 403–414.

Bowden, F. P. (1957). Adhesion and friction. *Endeavour* **16**, 5–18.

Brennan, E. B. and Weinbaum, S. E. (2001). Effect of epicuticular wax on adhesion of psyllids to glaucous juvenile and glossy leaves of *Eucalyptus globulus* Labillardière. *Aust. J. Ent.* **40**, 270–277.

Crisp, D. J. (1963). Waterproofing mechanisms in animals and plants. In *Waterproofing and Water-Repellency* (ed. L. L. Moilliet), pp. 416–481. Amsterdam: Elsevier.

Darnhofer-Demar, B. (1969). Zur Fortbewegung des Wasserläufers *Gerris lacustris* L. auf der Wasseroberfläche. *Zool. Anz. Suppl.* **32**, 430–439.

Denny, M. W. (1993). Surface tension: The energy of the interface. In *Air and Water: The Biology of Physics of Life's Media* (ed. M. W. Denny), pp. 253–270. Chichester: Princeton University Press.

Dixon, A. F. G., Croghan, P. C. and Gowing, R. P. (1990). The mechanism by which aphids adhere to smooth surfaces. *J. Exp. Biol.* **152**, 243–253.

Eigenbrode, S. D. (1996). Plant surface waxes and insect behaviour. In *Plant Cuticle* (ed. G. Kersteins), pp. 201–221. Oxford: BIOS Scientific Publishers.

Federle, W., Rohrseitz, K. and Hölldobler, B. (2000). Attachment forces of ants measured with a centrifuge: better 'wax-runners' have a poorer attachment to a smooth surface. *J. Exp. Biol.* **203**, 505–512.

Fogg, G. E. (1947). Quantitative studies on the wetting of leaves by water. *Proc. R. Soc. Lond. B* **134**, 503–522.

Fogg, G. E. (1948). Adhesion of water to the external surfaces of leaves. *Disc. Faraday Soc.* **3**, 162–166.

Freude, H., Harde, K. W. and Lohse, G. A. (1964). *Die Käfer Mitteleuropas. IV. Staphylinidae I.* Krefeld: Goecke & Evers. 264pp.

Gorb, S., Gorb, E. and Kastner, V. (2001). Scale effects on the attachment pads and friction forces in syrphid flies (Diptera, Syrphidae). *J. Exp. Biol.* **204**, 1421–1431.

Gorb, S. and Scherge, M. (2000). Biological microtribology: anisotropy in frictional forces of orthopteran attachment pads reflects the ultrastructure of a highly deformable material. *Proc. R. Soc. Lond. B* **267**, 1239–1244.

Guthrie, M. (1989). Animals of the surface film. In *Naturalists' Handbooks*, vol. 12 (ed. S. A. Corbet and R. H. L. Disney), pp. 1–87. Slough: The Richmond Publishing Co. Ltd.

Hasenfuss, I. (1999). The adhesive devices in larvae of Lepidoptera (Insecta, Pterygota). *Zoomorphology* **119**, 143–162.

Herman, L. H. (2001). Catalog of the Staphylinidae (Insecta: Coleoptera) 1758 to the end of the second millenium. IV. Staphylininae group (Part 1). *Bull. Am. Mus. Nat. Hist.* **265**, 1807–2440.

Holdgate, M. W. (1955). The wetting of insect cuticles by water. *J. Exp. Biol.* **32**, 591–617.

Horion, A. D. (1963). *Faunistik der Mitteleuropäischen Käfer Band. IX. Staphylinidae.* I. Teil. Überlingen-Bodensee: August Feyel. 412pp.

Ishii, S. (1987). Adhesion of a leaf feeding ladybird *Epilachna vigintioctomaculata* (Coleoptera: Coccinellidae) on a vertically smooth surface. *Appl. Ent. Zool.* **22**, 222–228.

Jenkins, M. F. (1960). On the method by which *Stenus* and *Dianous* (Coleoptera: Staphylinidae) return to the banks of a pool. *Trans. R. Ent. Soc. Lond.* **112**, 1–14.

Jiao, Y., Gorb, S. and Scherge, M. (2000). Adhesion measured on the attachment pads of *Tettigonia viridissima* (Orthoptera, Insecta). *J. Exp.Biol.* **203**, 1887–1895.

Juniper, B. E. and Burras, J. K. (1962). How pitcher plants trap insects. *New Sci.* **13**, 75–77.

Juniper, B. E. and Jeffree, C. E. (1983). *Plant Surfaces*. London: Edward Arnold. 93pp.

Koch, K. (1989). *Die Käfer Mitteleuropas Ökologie.* Band 1. Krefeld: Goecke & Evers. 440pp.

Kosaki, A. and Yamaoka, R. (1996). Chemical composition of footprints and cuticula lipids of three species of lady beetles. *Jpn. J. Appl. Entomol. Zool.* **40**, 47–53.

Lees, A. D. and Hardie, J. (1988). The organs of adhesion in the aphid *Megoura viciae*. *J. Exp. Biol.* **136**, 209–228.

Linsenmair, K. E. (1963). Eine bislang unbekannte Fortbewegungsart bei Insekten: Das Entspannungsschwimmen. *Kosmos* **59**, 331–334.

McFarlane, J. S. and Tabor, D. (1950). Adhesion of solids and the effect of surface films. *Proc. R. Soc. Lond. A* **202**, 224–243.

Møller Andersen, N. (1976). A comparative study of locomotion on the water surface in semiaquatic bugs (Insecta, Hemiptera, Gerromorpha). *Vidensk. Meddr Dansk Naturh. Foren.* **139**, 337–396.

Noble-Nesbitt, J. (1963). Transpiration in *Podura aquatica* L. (Collembola, Isotomidae) and the wetting properties of its cuticle. *J. Exp. Biol.* **40**, 681–700.

Owens, D. K. and Wendt, R. C. (1969). Estimation of the surface free energy of polymers. *J. Applied Polymer Sci.* **13**, 1741–1747.

Perssons, N. J. (1998). *Sliding Friction*. Berlin, Heidelberg: Springer. 462pp.

Puthz, V. (1971). Revision der afrikanischen Steninenfauna und Allgemeines über die Gattung *Stenus* Latreille (Coleoptera, Staphylinidae). *Annls. Mus. r. Afr. Cent. Ser. 8.* **187**, 1–376.

Rabel, W. (1971). Einige Aspekte der Benetzungstheorie und ihre Anwendung auf die Untersuchung und Veränderung der Oberflächeneigenschaften von Polymeren. *Farbe Lack* **77**, 997–1005.

Renkonen, O. (1934). Über das Vorkommen der *Stenus*-Arten (Col. Staph.) an verschiedenen Wohnorten in Finnland. *Ann. Zool. Soc-Bot. Fenn. Vanamo* **1**, 1–33.

Roth, L. M. and Willis, E. R. (1952). Tarsal structure and climbing ability of cockroaches. *J. Exp. Zool.* **119**, 483–517.

Scherge, M. and Gorb, S. (2001). *Biological Macro- and Nanotribology*. Springer: Berlin, Heidelberg. 304pp.

Sokal, R. R. and Rohlf, F. J. (1995). *Biometry*. New York: Freeman & Co. 887pp.

Stork, N. E. (1980a). Experimental analysis of *Chrysolina polita* (Chrysomelidae: Coleoptera) on a variety of surfaces. *J. Exp. Biol.* **88**, 91–107.

Stork, N. E. (1980b). A scanning electron microscope study of tarsal adhesive setae in the Coleoptera. *Zool. J. Linn. Soc.* **68**, 173–306.

Stork, N. E. (1980c). Role of waxblooms in preventing attachment to brassicas by the mustard beetle *Phaedon cochleariae*. *Ent. Exp. Appl.* **28**, 100–107.

Suter, R. B., Rosenberg, O., Loeb, S., Wildman, H. and Long, J. H. (1997). Locomotion on the water surface: propulsive mechanisms of the fisher spider *Dolomedes triton*. *J. Exp. Biol.* **200**, 2523–2538.

Suter, R. B. and Wildman, H. (1999). Locomotion on the water surface: hydrodynamic constraints on rowing velocity require a gait change. *J. Exp. Biol.* **202**, 2771–2785.

Walker, G., Yule, A. B. and Ratcliffe, J. (1985). The adhesive organ of the blowfly, *Calliphora vomitoria*: a functional approach (Diptera: Calliphoridae). *J. Zool., Lond. A* **205**, 297–307.

Weinreich, E. (1968). Über den Klebfangapparat der Imagines von *Stenus* LATR. (Coleopt., Staphylinidae) mit einem Beitrag zur Kenntnis der Jugendstadien dieser Gattung. *Z. Morph. Ökol. Tiere* **62**, 162–210.

Wigglesworth, V. B. (1987). How does a fly cling to the undersurface of a glass sheet? *J. Exp. Biol.* **129**, 373–376.

Wu, S. (1973). Polar and nonpolar interactions in adhesion. *J. Adhesion* **5**, 39–55.

Zar, J. H. (1999). *Biostatistical Analysis*. Upper Saddle Rier: Prentice Hall. 663pp.

Zisman, W. A. (1964). Relation of the equilibrium contact angle to liquid and solid constitution. In *Contact Angle, Wettability and Adhesion* (ed. F. M. Fowkes). *Adv. Chem. Ser.* **43**, 1–51. Washington: American Chemical Society.